# *Statistical correlations of nuclear quadrupole deformations and charge radii*

Paul-Gerhard Reinhard and Witold Nazarewicz

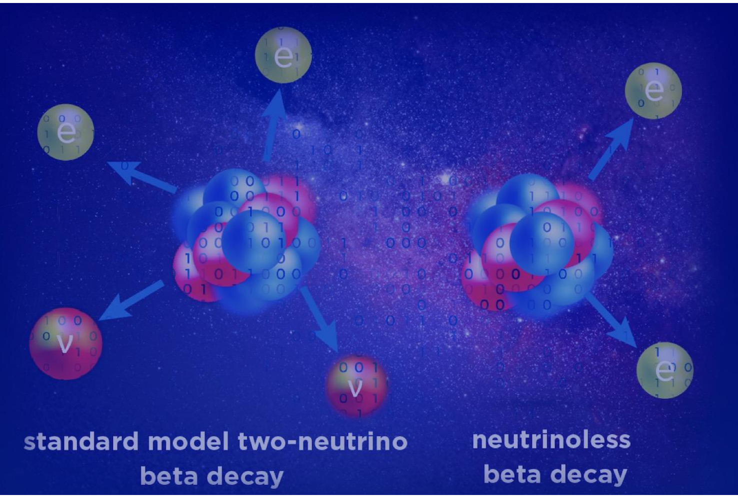


**Changfeng Jiao (焦长峰)**
**Shool of Physics and Astronomy**
**Sun Yat-Sen University**

Journal Club, June 21$^{st}$ @ Zhuhai, Guangdong

# Motivation

The purpose of this Paper: analyse the local trends of quadrupole deformations and charge radii in terms of statistical correlations between predicted observables in neighboring nuclei.

Occupations of s.p.levels change smoothly with *Z* and *N*, and the character of s. p. levels around the Fermi level is similar

→

Large statistical correlations between deformations and radii in close-lying isotopes and isotones.

Thus the trend of statistical correlations can

- indicates changes in shell structure.
- provide important information for modeling emulators based on machine learning.
- help assessing statistical errors on differences of observables.

# Theoretical models

The Skyrme force

$$\hat{H} = \sum_i \hat{t}_i + \sum_{i<j} v_{ij}^{(2)} + \sum_{i<j<k} v_{ijk}^{(3)}$$

The two-body interaction is given by

$$\begin{aligned} v_{12}^{(2)} = & t_0 \left(1 + x_0 \hat{P}_\sigma\right) \delta\left(r_1 - r_2\right) \\ & + \frac{1}{2} t_1 \left(\delta\left(\boldsymbol{r}_1 - \boldsymbol{r}_2\right) \hat{k}^2 + \hat{k}'^2 \delta\left(\boldsymbol{r}_1 - \boldsymbol{r}_2\right)\right) \\ & + t_2 \hat{\boldsymbol{k}} \cdot \delta\left(\boldsymbol{r}_1 - \boldsymbol{r}_2\right) \hat{\boldsymbol{k}}' + \mathrm{i} W_0 \left(\hat{\boldsymbol{\sigma}}_1 + \hat{\boldsymbol{\sigma}}_2\right) \cdot \hat{\boldsymbol{k}}' \times \delta\left(\boldsymbol{r}_1 - \boldsymbol{r}_2\right) \hat{\boldsymbol{k}} \end{aligned}$$

where $\hat{\boldsymbol{k}} = \frac{1}{2\mathrm{i}}\left(\vec{\nabla}_1 - \vec{\nabla}_2\right) \quad , \quad \hat{\boldsymbol{k}}' = -\frac{1}{2\mathrm{i}}\left(\overleftarrow{\nabla}_1 - \overleftarrow{\nabla}_2\right)$

The three-body interaction is given by

$$v_{123}^{(3)} = t_3 \delta\left(\boldsymbol{r}_1 - \boldsymbol{r}_2\right) \delta\left(\boldsymbol{r}_2 - \boldsymbol{r}3\right)$$

# Theoretical models

The Skyrme force parameter set:  SV-min

Fitting strategy:
The free parameters of the SHF ansatz are determined by a least-squares fit. Let us consider a model having $N_p$ parameters $p = (p_1, \ldots, p_{N_p})$ that are fitted to $N_d$ measured observables $\mathcal{O}_i$ $(i = 1, \ldots, N_d)$.

$$\chi^2(\boldsymbol{p}) = \sum_{i=1}^{N_d} \frac{\left(\mathcal{O}_i(\boldsymbol{p}) - \mathcal{O}_i^{\exp}\right)^2}{\Delta\mathcal{O}_i^2}$$

The adopted errors are determined as follows.

$$\Delta\mathcal{O}_i^2 = \left(\Delta\mathcal{O}_i^{\exp}\right)^2 + \underbrace{\boxed{\left(\Delta\mathcal{O}_i^{\mathrm{num}}\right)^2}}_{\text{usually small}} + \boxed{\left(\Delta\mathcal{O}_i^{\mathrm{the}}\right)^2}$$

How to determine $\Delta\mathcal{O}_i^{\mathrm{the}}$

in the case of statistical fluctuations there is a consistency between the distribution of residuals and the adopted error. Namely, the rules of statistical analysis require that the total penalty function at the minimum should be normalized to $N_d - N_p$

$$\Rightarrow \quad \frac{\chi^2(\boldsymbol{p}_0)}{N_d - N_p} \longleftrightarrow 1. \quad \Rightarrow \quad \sum_{i \in \mathrm{typ}} \frac{\left(\mathcal{O}_i(\boldsymbol{p}) - \mathcal{O}_i^{\exp}\right)^2}{\Delta\mathcal{O}_i^2} = N_{\mathrm{typ}} \frac{N_d - N_p}{N_d},$$

# Theoretical models

The Skyrme force parameter set: SV-min

one needs to confine the model space to a "physically reasonable" domain around the minimum $p_0$. we can expand $\chi^2$ as

$$\chi^2(\boldsymbol{p}) - \chi_0^2 \approx \sum_{\alpha,\beta=1}^{N_p} (p_\alpha - p_{0,\alpha}) \mathcal{M}_{\alpha\beta} (p_\beta - p_{0,\beta}),$$

$$\mathcal{M}_{\alpha\beta} = \frac{1}{2} \partial_{p_\alpha} \partial_{p_\beta} \chi^2 \Big|_{\boldsymbol{p}_0},$$

The adopted errors are determined as follows.

$$(\boldsymbol{p} - \boldsymbol{p}_0) \hat{\mathcal{M}} (\boldsymbol{p} - \boldsymbol{p}_0) \leqslant 1,$$

in the case of statistical fluctuations there is a consistency between the

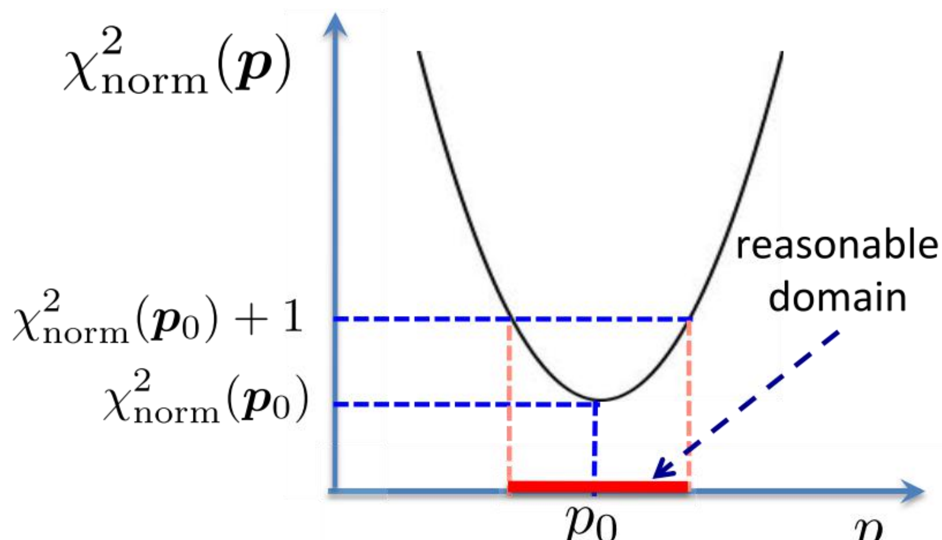

# Theoretical models

I. Skyrme force parameter set: SV-min

P. Klupfel et. al., PRC 79, 034310 (2009).

TABLE I. Global quality measures for various classes of observables as achieved with the parameterization SV-min. The second column shows the contribution from an observable to $\chi^2$ while the third column expresses this as $\chi^2$ per data point. The last column produces the r.m.s. errors as such and the numbers in brackets indicate the adopted error taken as weights for the fit; see Eq. (5).

| | $\chi^2$ | $\chi^2$/point | r.m.s. error | |
|---|---|---|---|---|
| Binding energy $E_B$ | 12.07 | 0.17 | 0.62 MeV | (1.0) |
| Diffr., radius $R$ | 11.18 | 0.40 | 0.029 fm | (0.04) |
| Surface thick. $\sigma$ | 4.22 | 0.26 | 0.022 fm | (0.04) |
| r.m.s. radius $r$ | 15.86 | 0.32 | 0.014 fm | (0.02) |
| Pairing gap $\Delta_p$ | 4.27 | 0.25 | 0.11 MeV | (0.12) |
| Pairing gap $\Delta_n$ | 2.43 | 0.15 | 0.14 MeV | (0.12) |
| l·s splitting | 3.18 | 0.45 | 0.25% | (20) |
| Total | 53.22 | 0.26 | | |

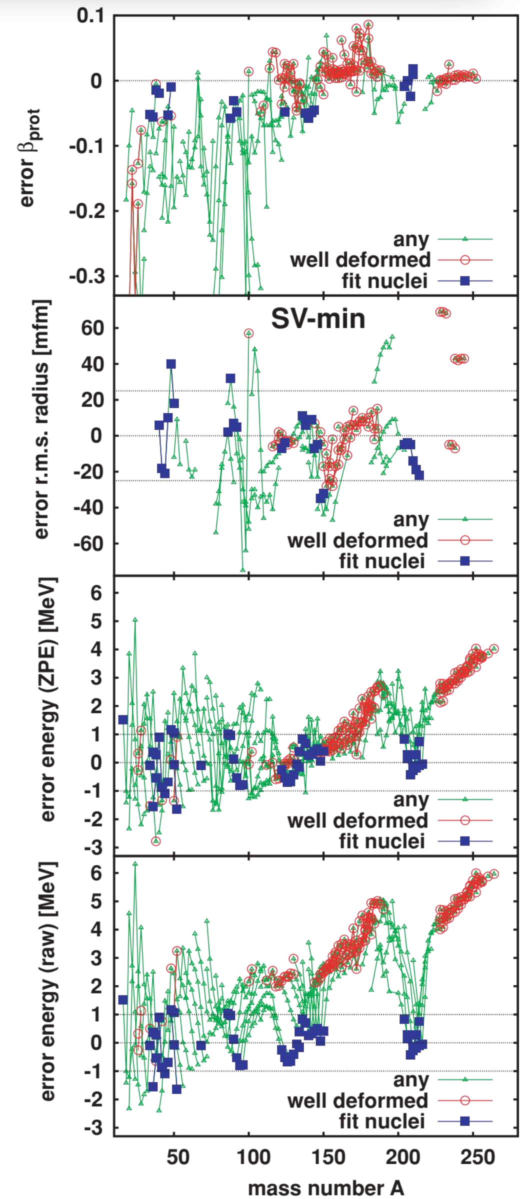

# Theoretical models

II. Fayans and Skyrme energy density functionals: $\mathrm{Fy}(\Delta r,\mathrm{BCS})$

P.-G. Reinhard and W. Nazarewicz, PRC 95, 064328 (2017).

*"The Fayans pairing functional, with its generalized density dependence, significantly improves the description of charge radii in odd and even nuclei."*

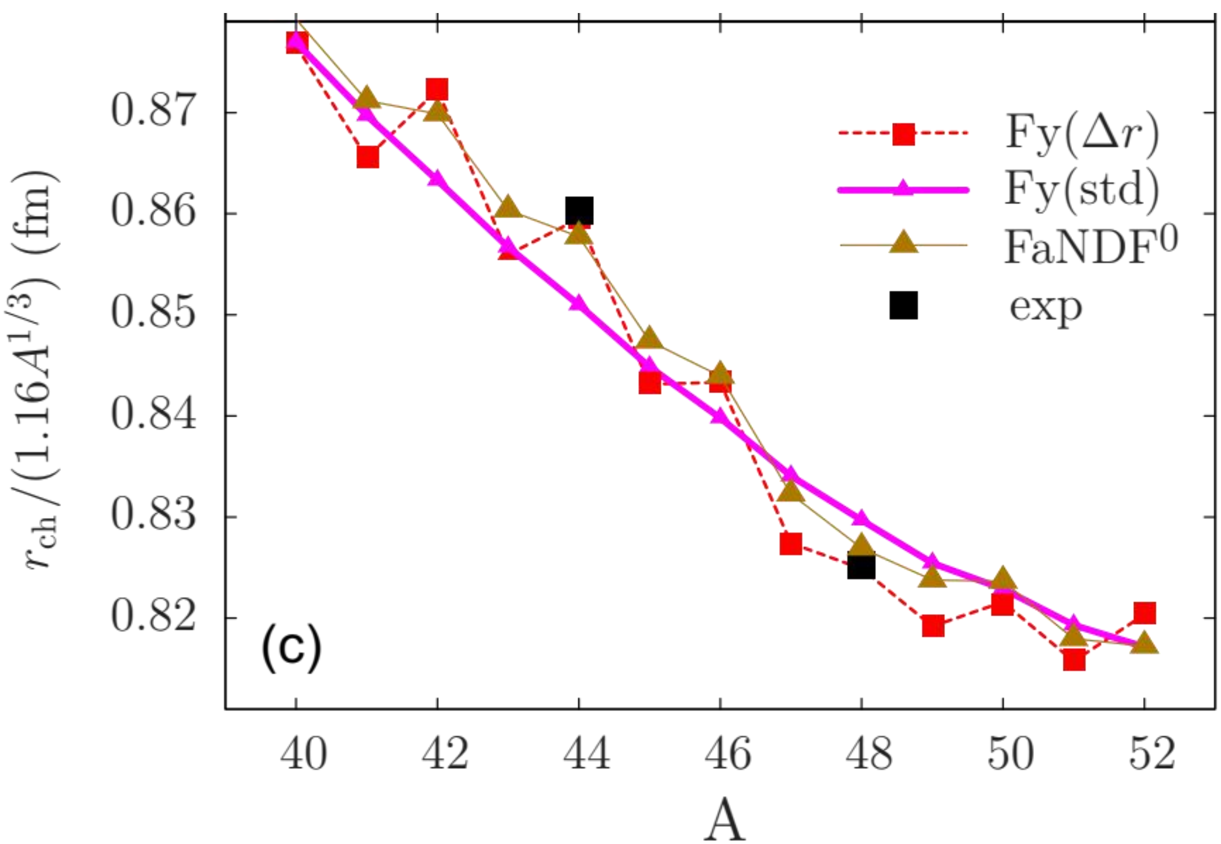

# Theoretical models

The Skyrme force parameter set:  SV-min

Statistical error:
Given a set of parameters *p*, any observable *A* can be within the model uniquely computed as *A* = *A*(*p*). The value of *A* thus varies within the confidence ellipsoid, and this results in some uncertainty *ΔA* of *A*.

$$A(\boldsymbol{p}) \simeq A_0 + \boldsymbol{G}^A \cdot (\boldsymbol{p} - \boldsymbol{p}_0) \quad \text{for} \quad A_0 = A(\boldsymbol{p}_0) \quad \text{and} \quad \boldsymbol{G}^A = \boldsymbol{\partial}_{\boldsymbol{p}} A\big|_{\boldsymbol{p}_0}.$$

The prescription for assigning an error to $A(p_0)$ is the following formula

$$\overline{\Delta A^2} = \sum_{\alpha\beta} G^A_\alpha \hat{\mathcal{C}}_{\alpha\beta} G^A_\beta,$$

where $\hat{\mathcal{C}}$ is the covariance matrix

$$\hat{\mathcal{C}} = \hat{\mathcal{M}}^{-1} = \left(\hat{J}^T \hat{J}\right)^{-1}$$

where

$$\hat{J}_{i\alpha} = \frac{\partial_{p_\alpha} \mathcal{O}_i\big|_{\boldsymbol{p}_0}}{\Delta \mathcal{O}_i}$$

is the Jacobian matrix, which is inversely proportional to the adopted errors.

# Statistical correlation analysis

A weighted average over the parameter space yields the covariance between two observables $\hat{A}$ and $\hat{B}$, which represents their combined uncertainty:

$$\overline{\Delta A\, \Delta B} = \sum_{\alpha\beta} G_{\alpha}^{A} \hat{\mathcal{C}}_{\alpha\beta} G_{\beta}^{B}.$$

In addition, one can introduce a useful dimensionless product–moment correlation coefficient

$$c_{AB} = \frac{|\overline{\Delta A\, \Delta B}|}{\sqrt{\overline{\Delta A^2}\ \overline{\Delta B^2}}}.$$

in this paper, $R_{x,y} = \dfrac{\mathrm{cov}(x,y)}{\sigma_x \sigma_y}$,

Positive covariance: Indicates that two variables tend to move in the same direction.
Negative covariance: Reveals that two variables tend to move in inverse directions.

The square $R^2$ is the coefficient of determination (**CoD**). It contains information on how well one quantity is determined by another one, within a given model.

$$0 < R^2 < 1$$

$R^2 = 0$: the quantities x and y are uncorrelated.
$R^2 = 1$: one quantity determines the other completely.

# Statistical correlation analysis

The square $R^2$ is the coefficient of determination (**CoD**). It contains information on how well one quantity is determined by another one, within a given model.

$$0 < R^2 < 1$$

$R^2 = 0$: the quantities x and y are uncorrelated.
$R^2 = 1$: one quantity determines the other completely.

The correlation coefficient is useful when estimating the variance of a difference $x - y$

$$\sigma_{x-y}^2 = \sigma_x^2 + \sigma_y^2 - 2R_{x,y}\sigma_x\sigma_y$$

If $R_{x,y} \approx 1$, then

$$\sigma_{x-y} \approx |\sigma_x - \sigma_y|$$

# Calculated quadrupole deformations

$$\beta_2 = 4\pi \frac{\langle r^2 Y_{20} \rangle}{3ZR^2}, \quad R = 1.2A^{1/3}\mathrm{fm}$$

Calculated values of $\beta_2$ for SV-min and Fy(Δr,BCS) and compares them to empirical quadrupole deformations extracted from the experimental transition probabilities for the lowest $2^+$ states.

Nuclear deformation properties are dominated by shell topology: all reasonable nuclear models, including macroscopic-microscopic approaches as well as various flavors of nuclear density functional method, are bound to reproduce the deformations of well deformed nuclei.

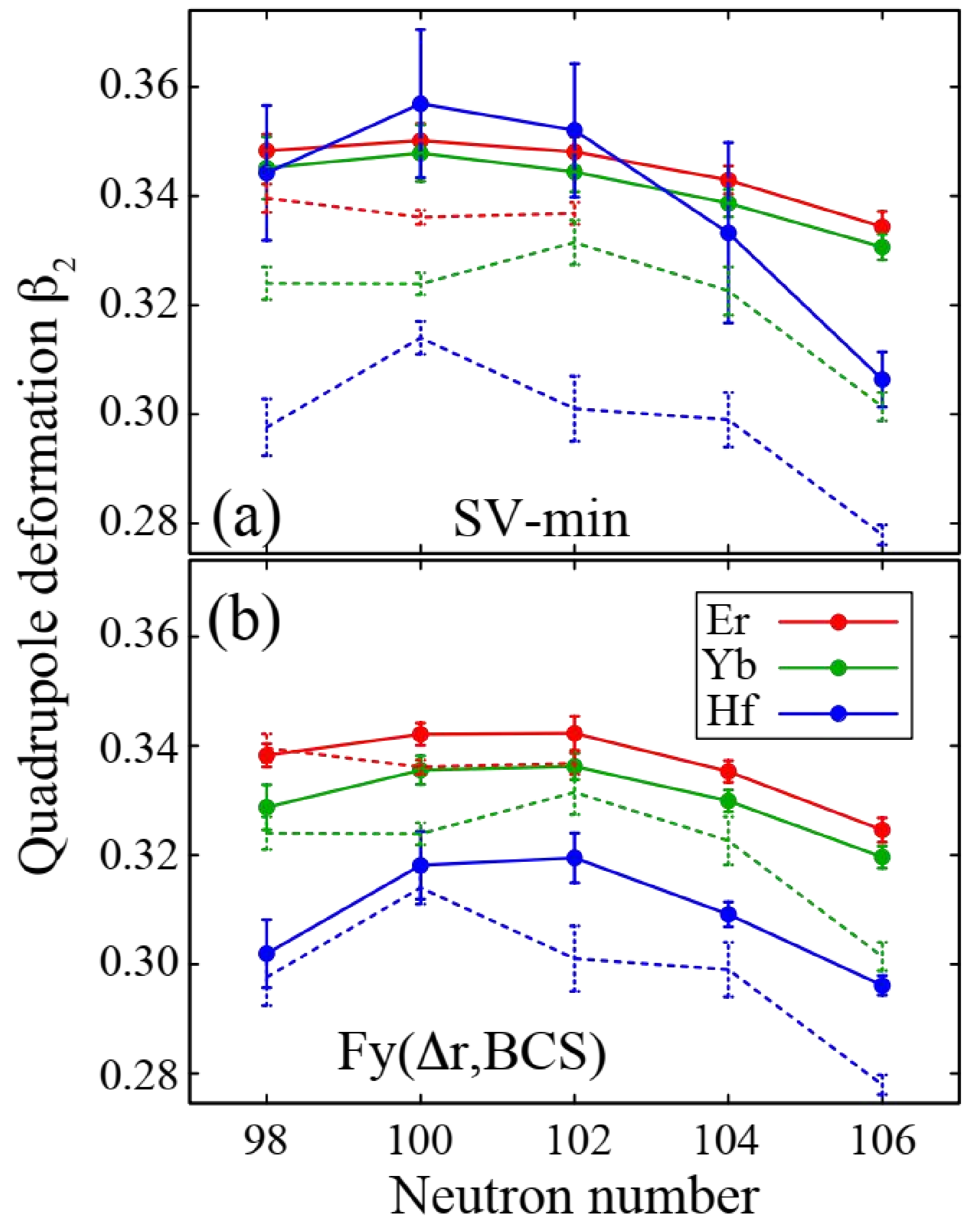

# Calculated quadrupole deformations

The values of $\beta_2$ predicted by SV-min are 5%-10% larger and the trend for the Hf isotopes differs visibly.

Although the deformation is dominated by shell structure, the final details emerge from an interplay of Coulomb pressure, surface energy, shell effects, and pairing, which all depend on the actual model.

Coulomb pressure and surface energy change only smoothly with $Z$ and $N$ and this should lead to strong inter-correlations. However, shell structure and pairing can fluctuate.

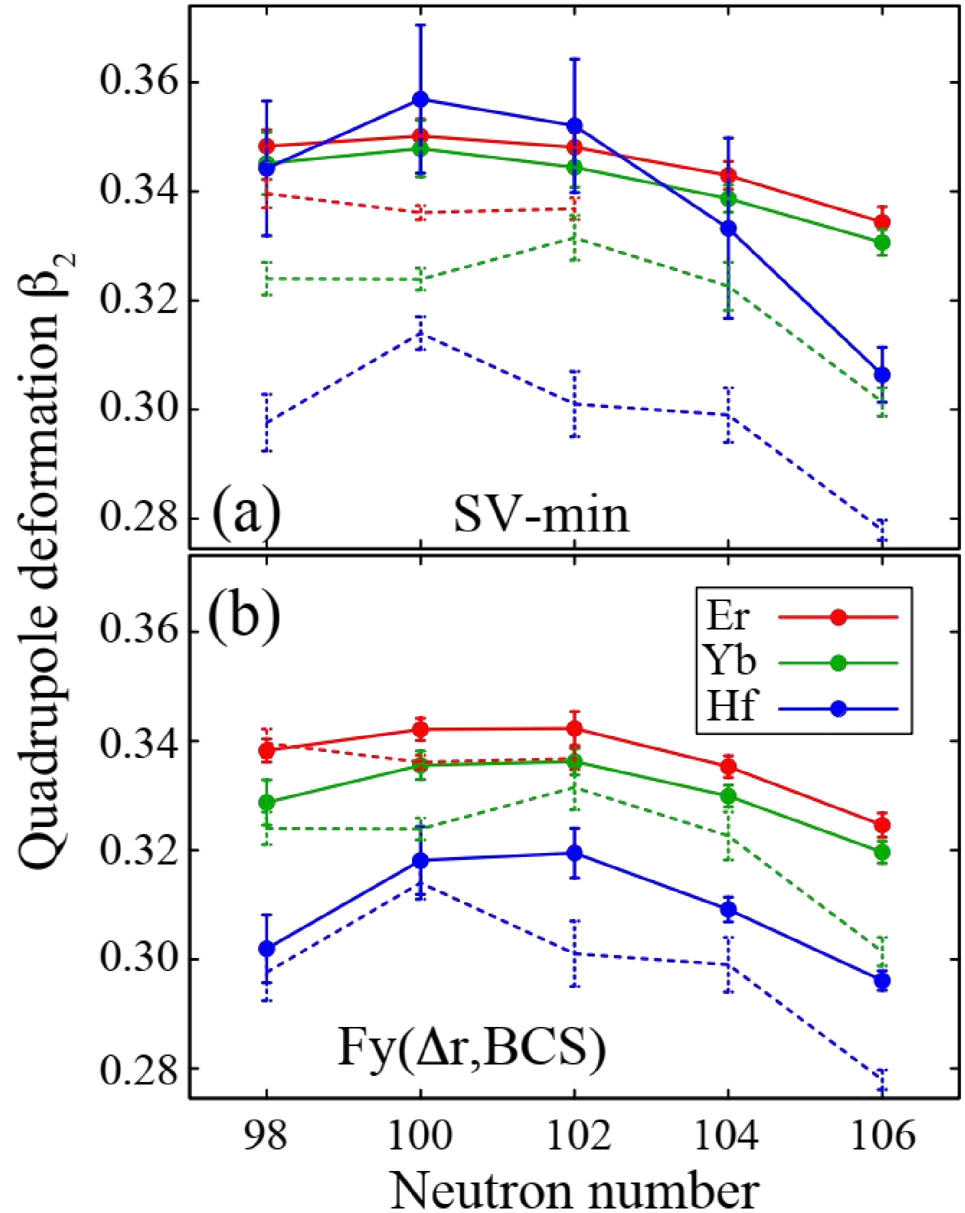

# Calculated charge radii

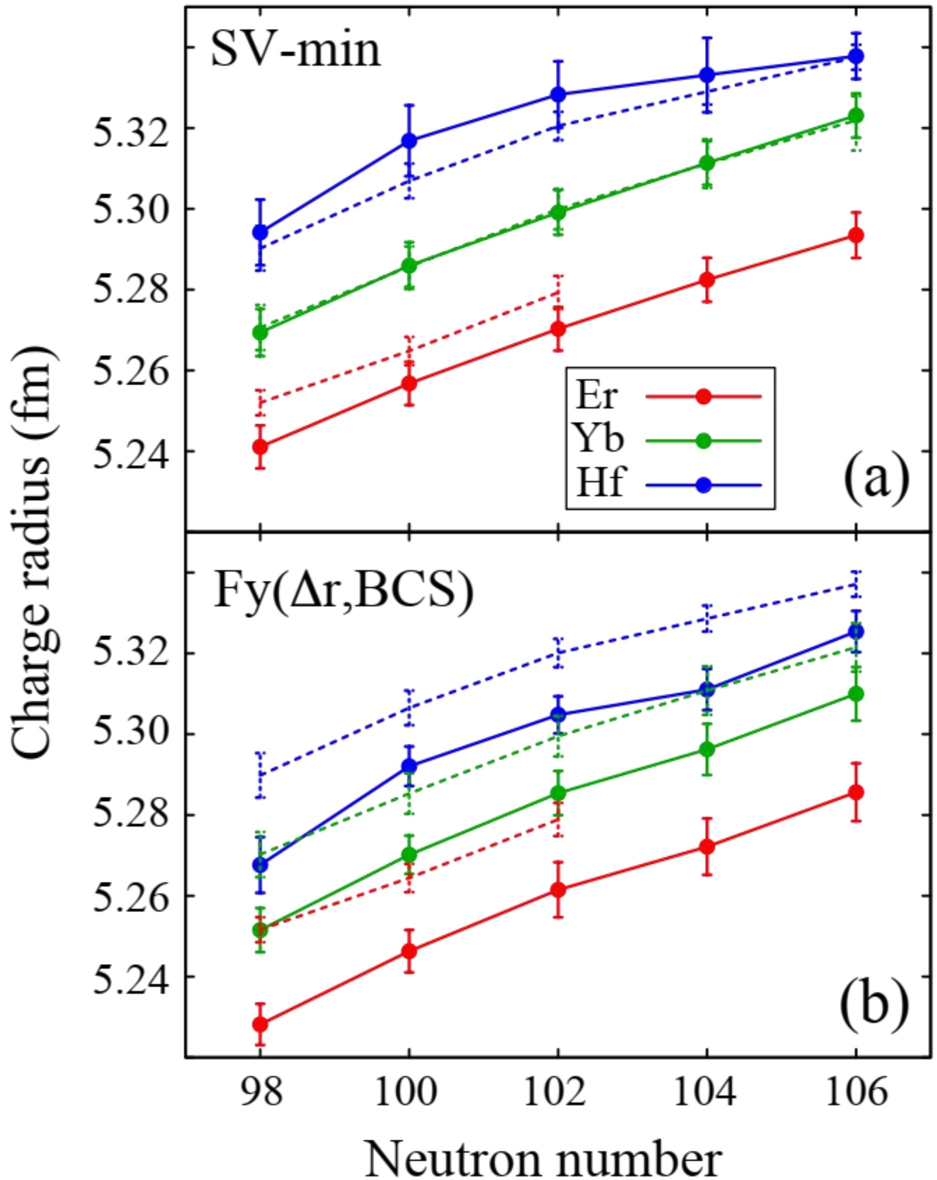


The charge radii Rch of the discussed Er, Yb, and Hf isotopes are displayed in Fig. 2. The radii gradually increase with Z and N, as expected. The fluctuations atop this smooth behavior are seen in the differential radii and their ratios. The charge radii obtained in SVmin are systematically larger than those of Fy(Δr,BCS). This, together with the results for the quadrupole moments shown in Fig. 1 suggests that the proton densities predicted by SV-min are slightly more radially extended.

# Statistical correlations between the deformations

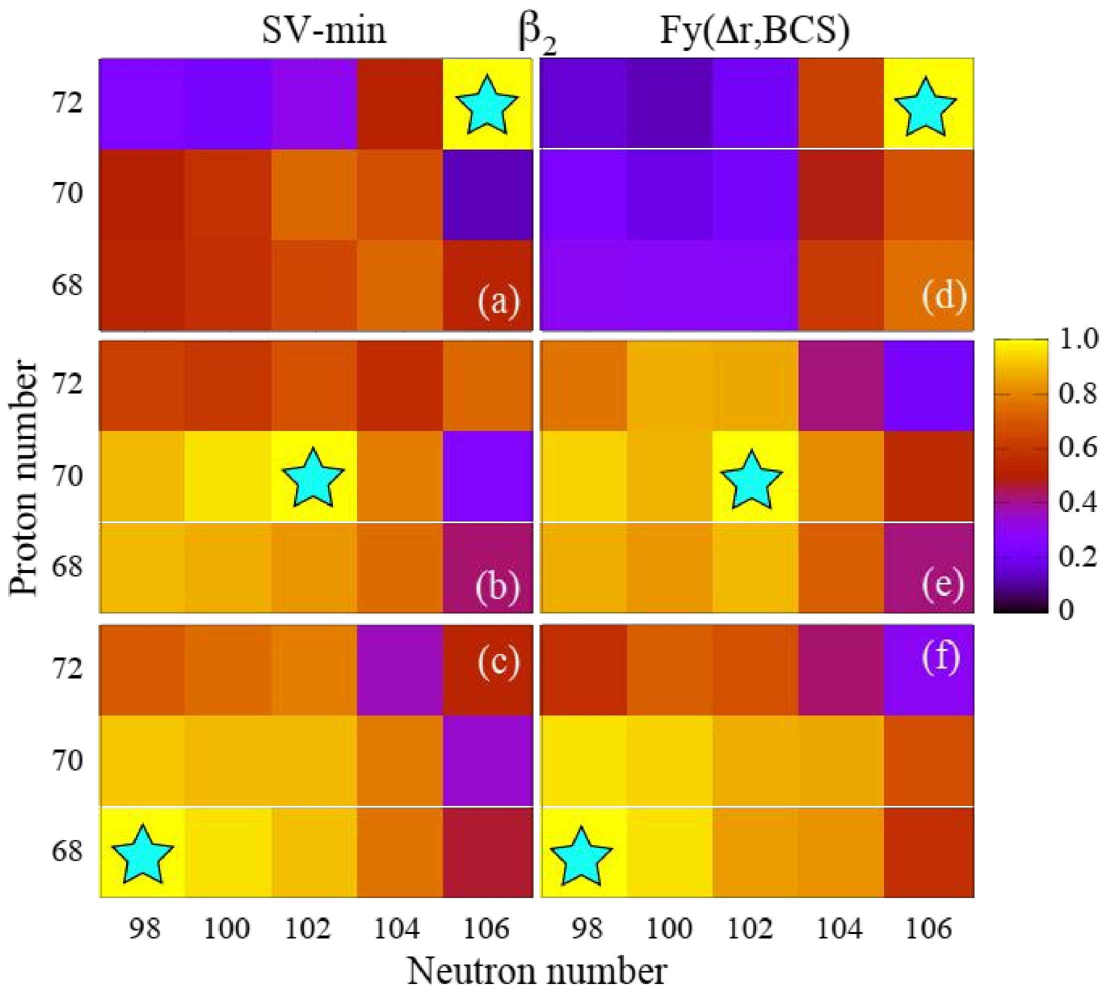


CoDs between the deformation $\beta_2$ in $^{178}$Hf (upper panels), $^{172}$Yb (middle panels), and $^{166}$Er (lower panels) and $\beta_2$ values of all other isotopes. The reference nucleus is indicated in each panel by a star. Interestingly, the quadrupole deformations of $^{172}$Yb ($N$ = 102) and $^{166}$Er ($N$ = 98) are well correlated with those of neighboring nuclei, in accordance with expectations. It i only when the neutron number approaches $N$= 106 that the correlation deteriorates. The situation is different for $^{178}$Hf. Here, the CoD values are small, even with the nearest neighbors.

# Statistical correlations between the charge radii

The inter-nuclei correlations of charge radii.
It is seen that the values of $R_{ch}$ are intercorrelated better than quadrupole deformations. But, similar as in the $\beta_2$ case, there are regions of surprisingly low CoDs. Particularly low correlations are predicted for $^{176}$Hf in SV-min and $^{170}$Hf in Fy(Δr,BCS) for both $\beta_2$ and $R_{ch}$

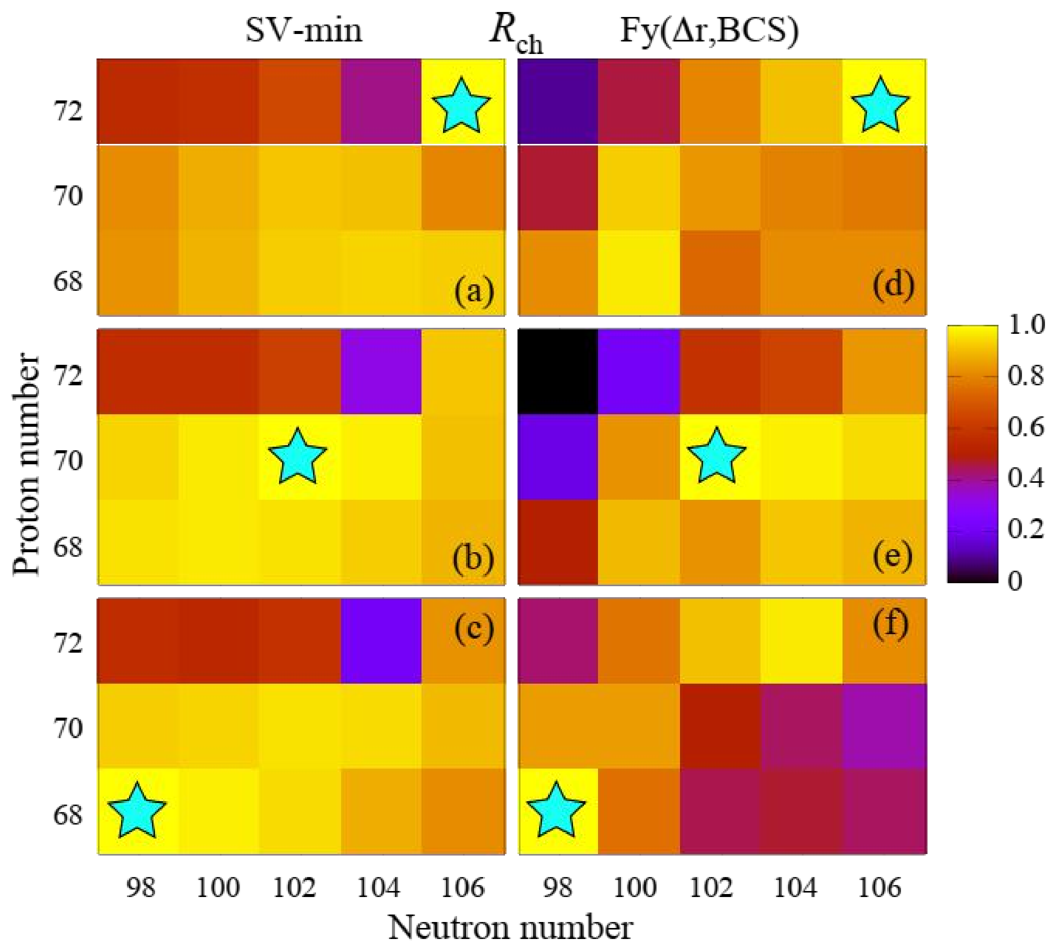


**The significant variations of CoDs are indicative of shell effects.**

# Nilsson Diagram (s. p. energies)

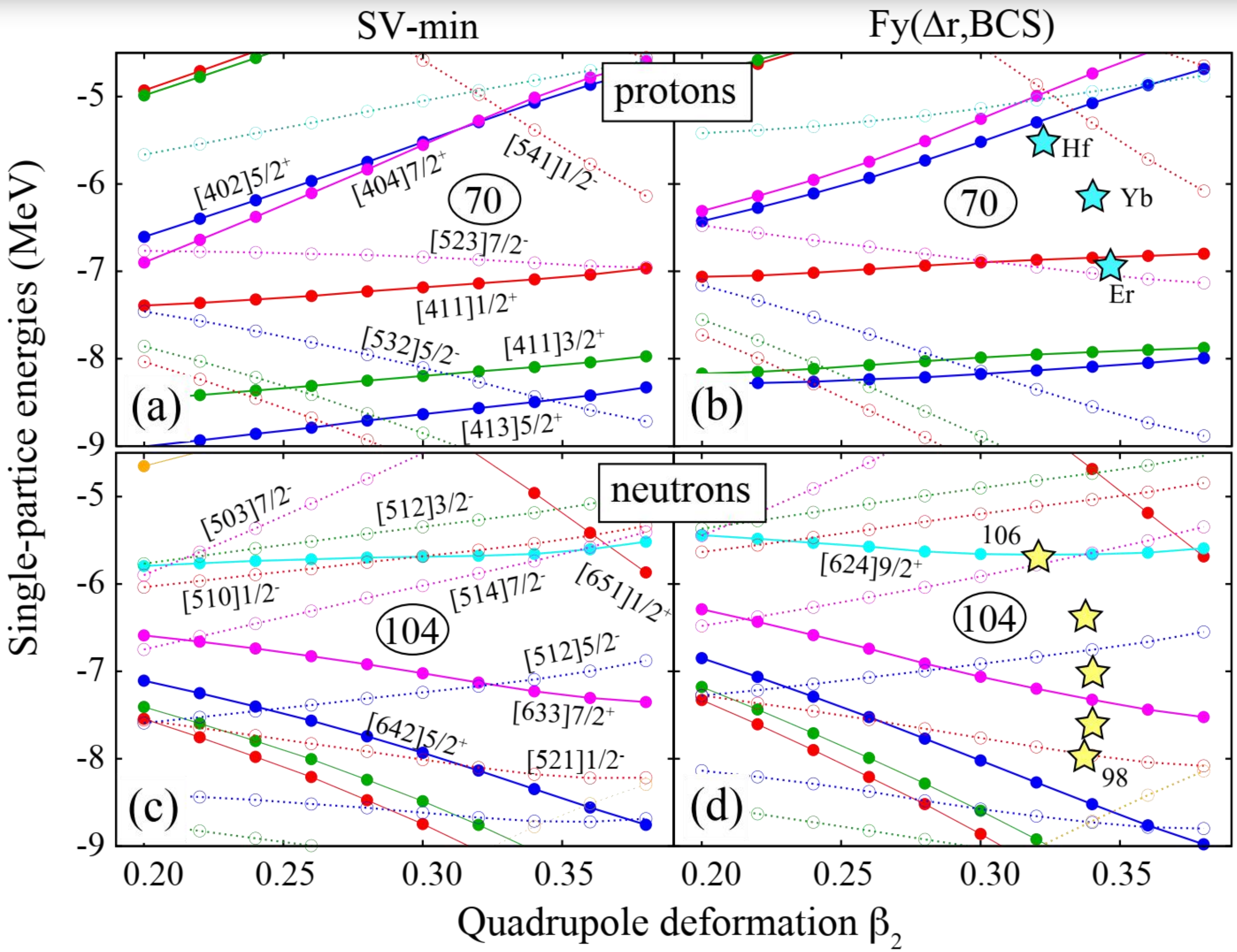


IG. 5. Proton (top) and neutron (bottom) single-particle energies of $^{172}$Yb calculated with SV-min (left) and Fy($\Delta r$,BCS) ight) EDFs. The asymptotic Nilsson labels $[N_{\rm osc} n_z \Lambda]\Omega^\pi$ are marked. The positions of proton Fermi levels for the $N = 102$ otones is indicated by stars in panel (b) and the neutron Fermi levels along the Yb isotopic chain - in panel (d).

# Nilsson Diagram (s. p. energies)

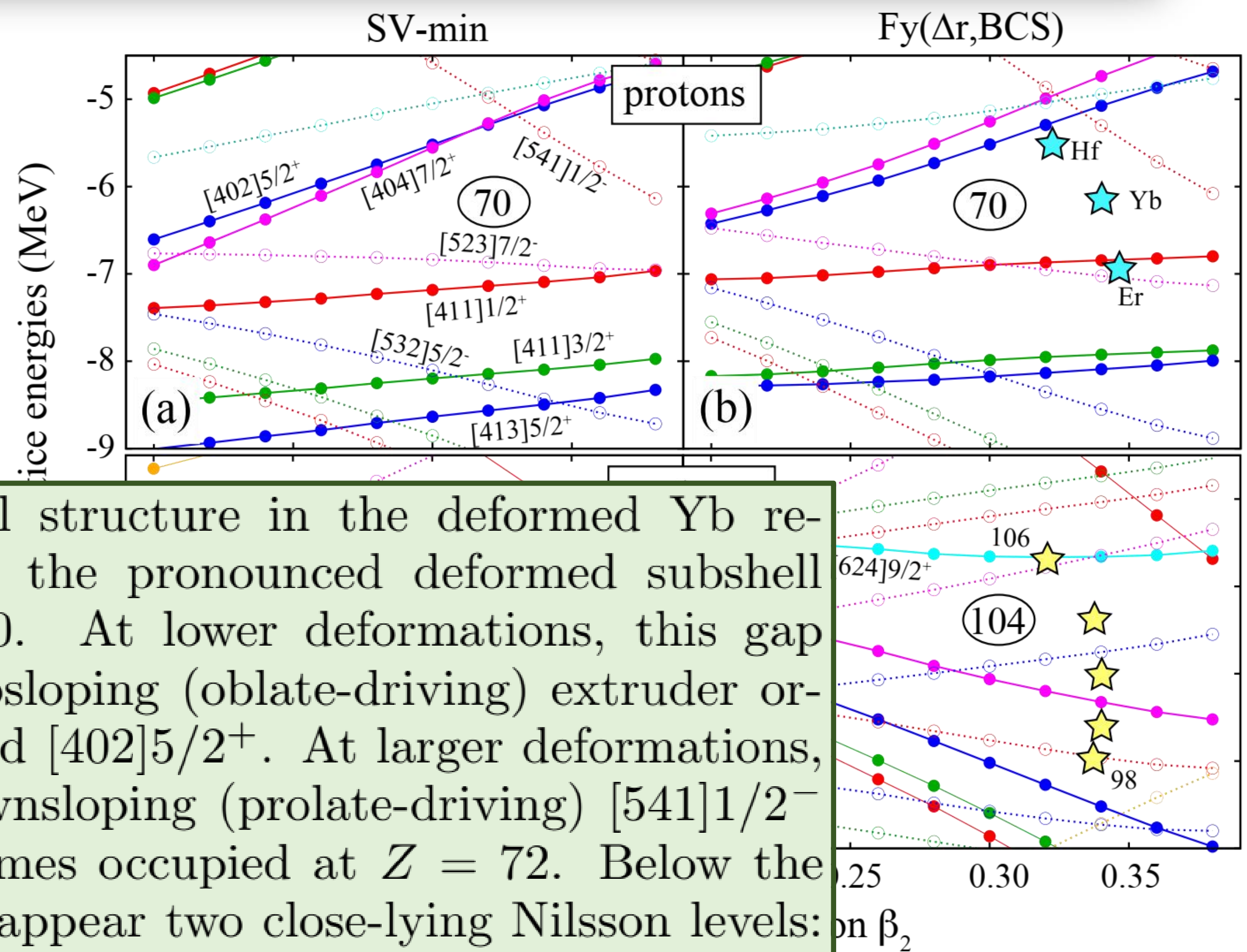


ated with SV-min (left) and Fy($\Delta r$,BCS)
ns of proton Fermi levels for the $N = 102$
isotopic chain - in panel (d).

The proton shell structure in the deformed Yb region is defined by the pronounced deformed subshell closure at $Z = 70$. At lower deformations, this gap is closed by the upsloping (oblate-driving) extruder orbitals $[404]7/2^+$ and $[402]5/2^+$. At larger deformations, $\beta_2 > 0.33$, the downsloping (prolate-driving) $[541]1/2^-$ intruder level becomes occupied at $Z = 72$. Below the $Z = 70$ gap, there appear two close-lying Nilsson levels: oblate-driving $[411]1/2^+$ and prolate-driving $[532]7/2^-$, which close another deformed gap at $Z = 66$. These levels cross at $\beta_2 \approx 0.30$ for Fy($\Delta r$,BCS) and $\beta_2 \approx 0.39$ for SV-min.

# Nilsson Diagram (s. p. energies)

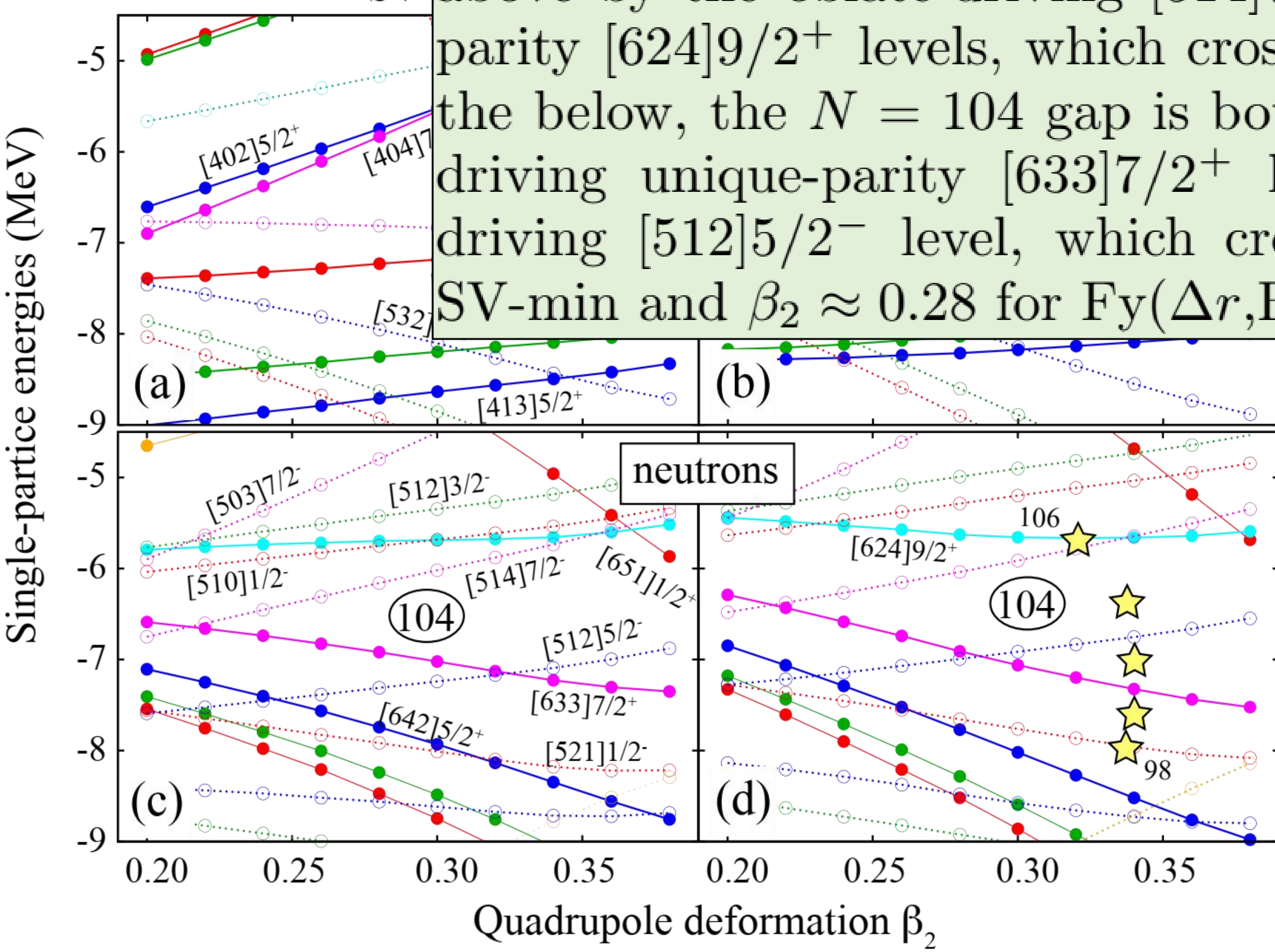


The neutron shell structure is characterized by the deformed gap at $N = 104$. This gap is closed from the above by the oblate-driving $[514]7/2^-$ and the unique-parity $[624]9/2^+$ levels, which cross at $\beta_2 \approx 0.35$. From the below, the $N = 104$ gap is bounded by the prolate-driving unique-parity $[633]7/2^+$ level and the oblate-driving $[512]5/2^-$ level, which cross at $\beta_2 \approx 0.32$ for SV-min and $\beta_2 \approx 0.28$ for Fy($\Delta r$,BCS).

# Pairing effects

*In the presence of nucleonic pairing, the s.p. occupations change gradually with particle number leading to smooth variations of nuclear observables. If pairing is weak, the transitions between intrinsic HF configurations are sharp and the underlying picture becomes diabatic. Consequently, large pairing is expected to increase correlations between observables belonging to different nuclei.*

The large deformed gap at $Z = 70$ gives rise to very weak proton pairing in the Yb isotopes. The variations of neutron pairing are appreciable; they reach a minimum at the deformed neutron closure $N = 104$.

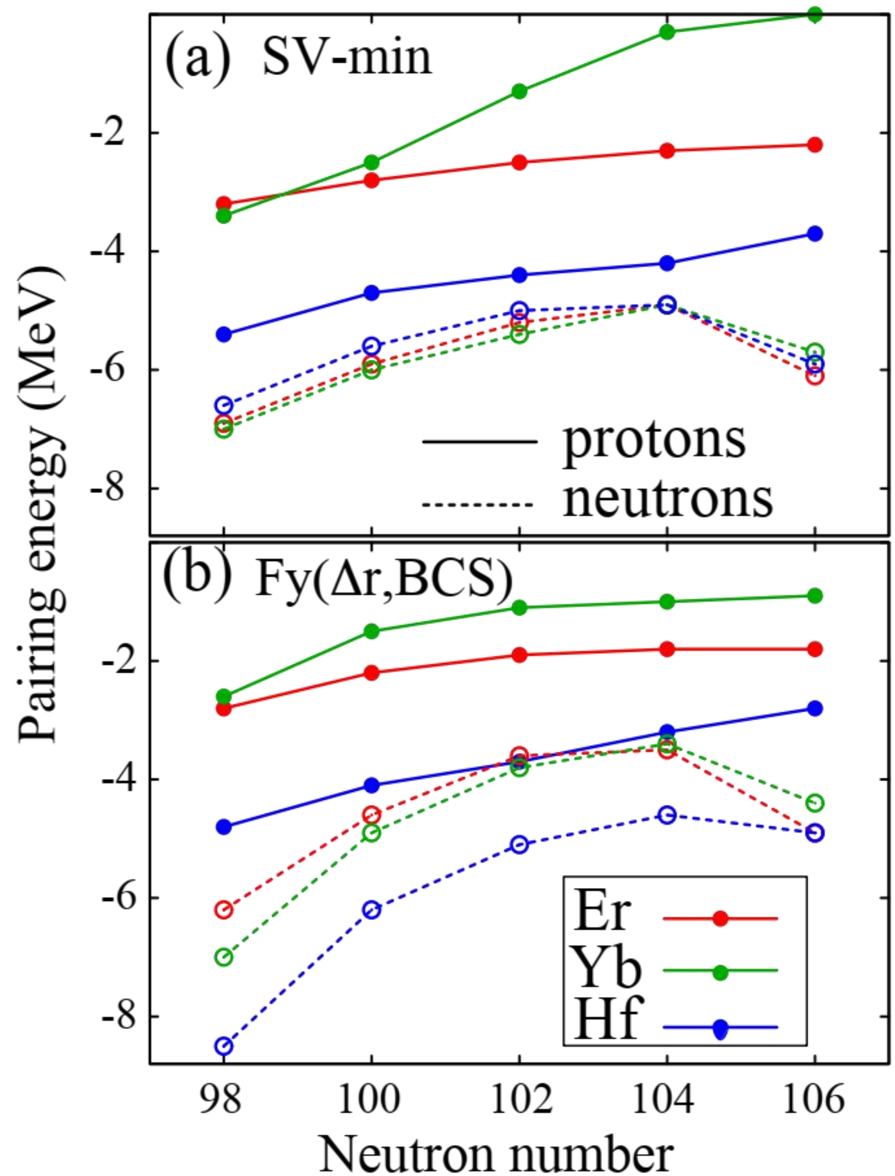

# Nilsson Diagram (s. p. energies)

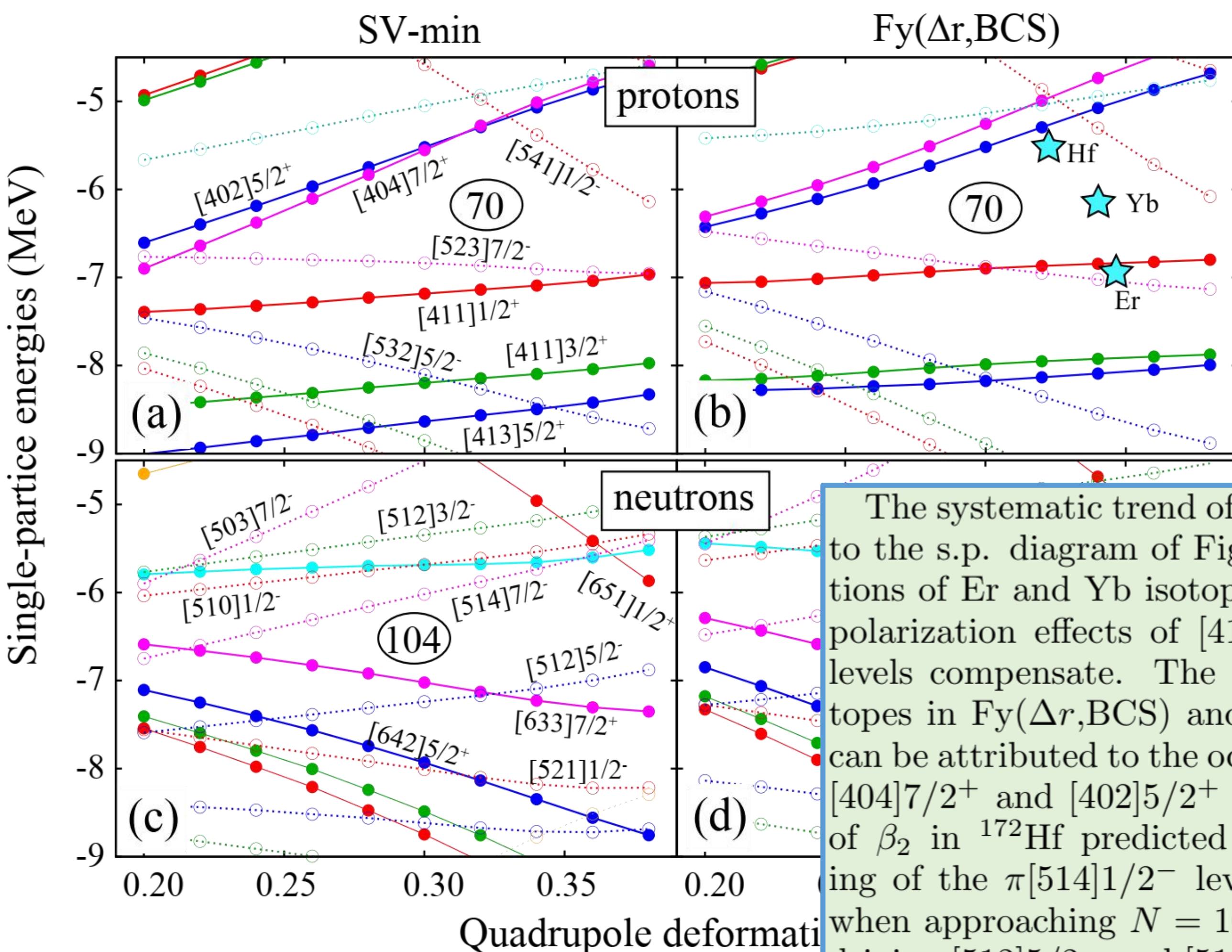


The systematic trend of $\beta_2$ in Fig. 1 can be traced back to the s.p. diagram of Fig. 5. The quadrupole deformations of Er and Yb isotopes are close as the quadrupole polarization effects of $[411]1/2^+$ and $[523]7/2^-$ proton levels compensate. The reduction of $\beta_2$ in the Hf isotopes in Fy($\Delta r$,BCS) and for $N > 100$ in Fy($\Delta r$,BCS) can be attributed to the occupations of the oblate-driving $[404]7/2^+$ and $[402]5/2^+$ proton levels. The large value of $\beta_2$ in $^{172}$Hf predicted in SV-min is due to the filling of the $\pi[514]1/2^-$ level. Finally, a reduction of $\beta_2$ when approaching $N = 106$ reflects the filling of oblate-driving $[512]5/2^-$ and $[514]7/2^-$ neutron levels. When it comes to the charge radii, the local increase of $R_{\rm ch}$ around $N = 100, 102$ can be associated with the occupation of the neutron intruder level $[633]7/2^+$.

# Nilsson Diagram (s. p. energies)

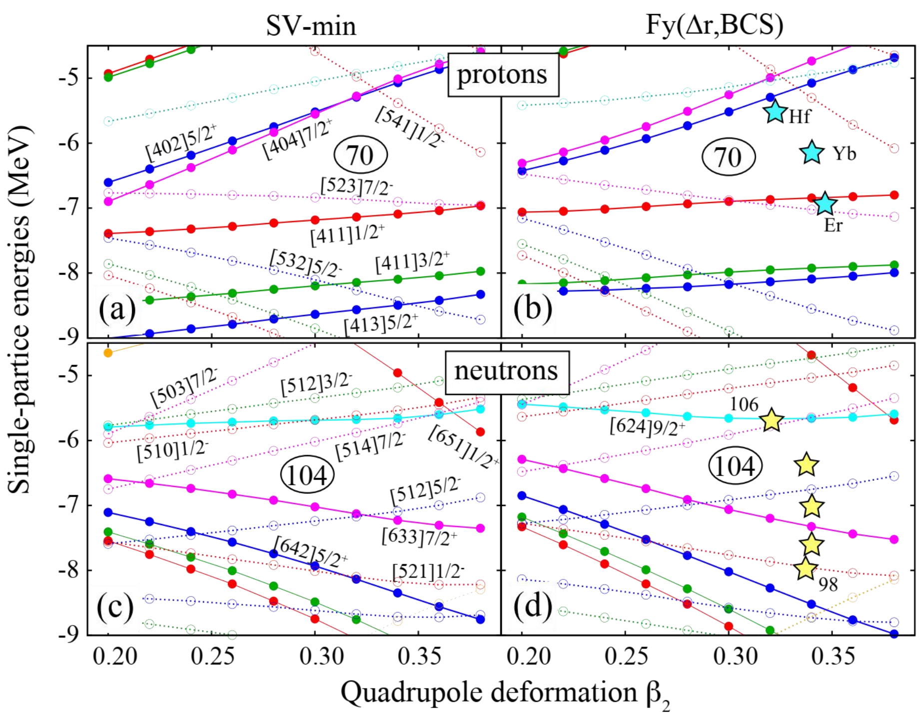


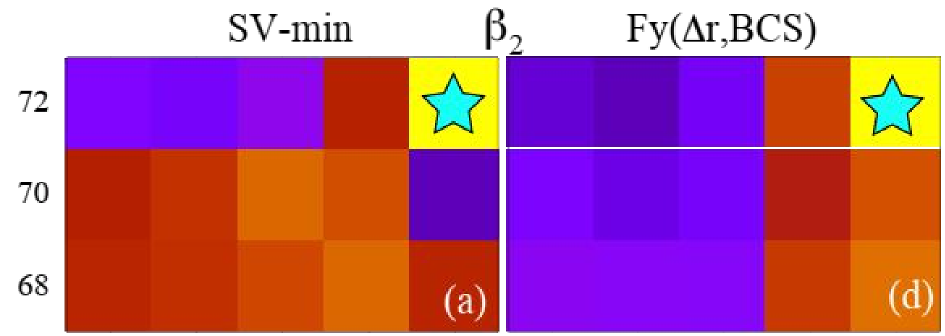


Let us begin discussion from the CoD pattern of $\beta_2$. As seen in Figs. 3(a) and 3(d), $\beta_2$ in $^{178}$Hf is poorly correlated with quadrupole deformations of other nuclei. This nucleus is predicted to have a reduced value of $\beta_2 \approx 0.3$ compared to other systems. At this deformation, the last two protons of $^{178}$Hf occupy the $[404]7/2^+$ and $[402]5/2^+$ extruder orbits, which are practically empty in the Yb and Er isotopes, as well as in $^{170,172,174}$Hf in SV-min in which the intruder level $[541]1/2^-$ becomes occupied at $\beta_2 > 0.34$. Moreover, the neutron structure of $^{178}$Hf involves the occupation of the $[514]7/2^-$ and $[624]9/2^+$ orbitals, which are empty in lighter isotopes with $N < 104$. All these configuration changes involve deformation-driving orbitals and result in reduced CoD values.

# Nilsson Diagram (s. p. energies)

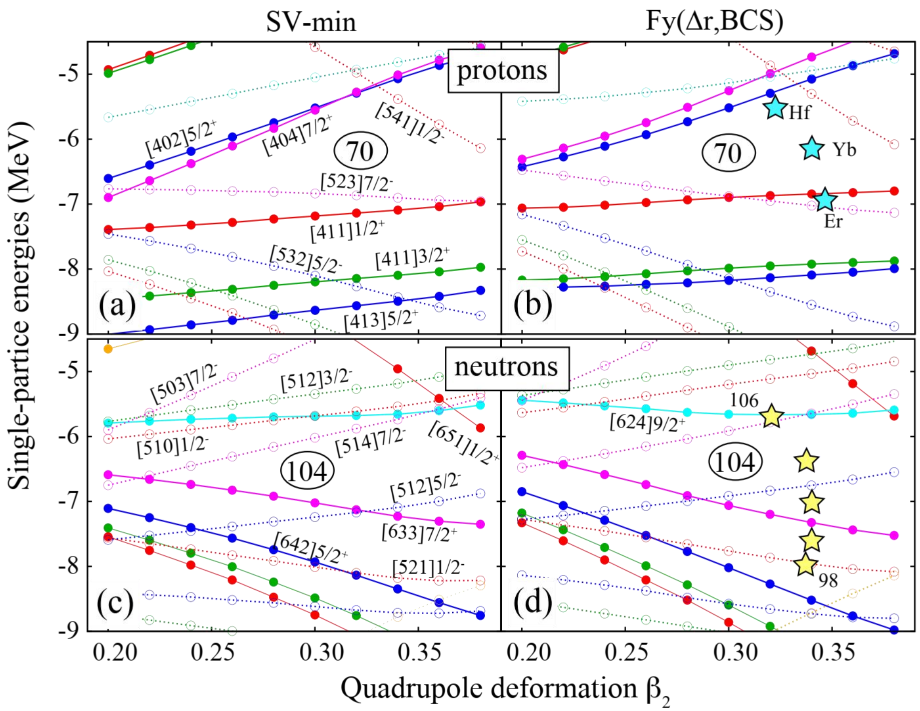


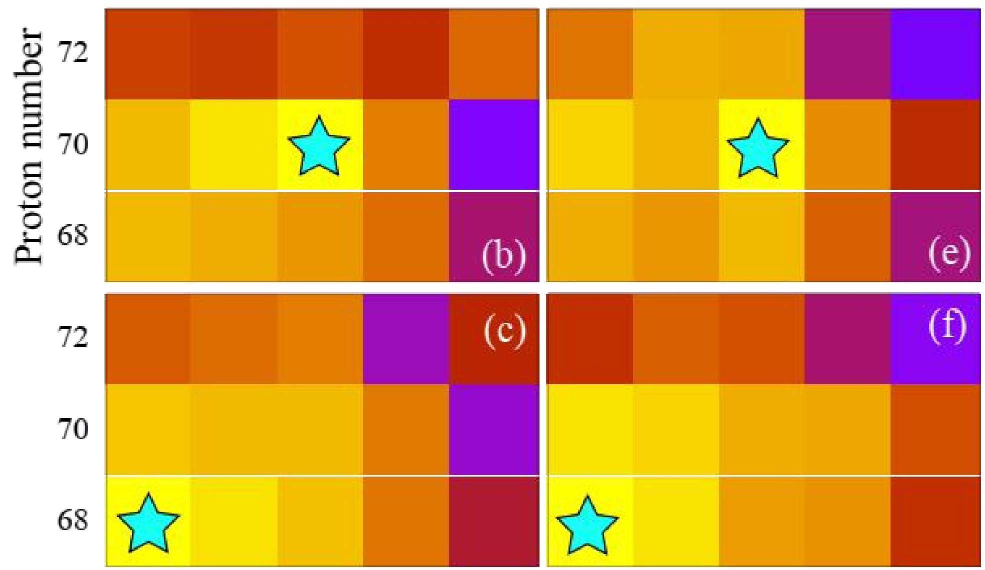


Moving on to Figs. 3(b) and 3(e), the quadrupole deformation of $^{172}$Yb is correlated fairly well with the $\beta_2$ values of lighter systems. This nucleus is calculated to have $\beta_2 \approx 0.34$. The decrease of correlations at $N = 106$ can be associated with the filling of the neutron $[624]9/2^+$ intruder level. The situation shown in Figs. 3(c) and 3(f) for $^{166}$Er is reminiscent of that for $^{172}$Yb: the decrease of $\beta_2$-correlations is seen for $N = 106$ (neutron $[624]9/2^+$ occupation) and $Z = 72$ (proton $[541]1/2^-$ or $[404]7/2^+/[402]5/2^+$ occupation).

# Summary

This paper investigated inter-correlations between observables in neighboring nuclei which exhibit smooth trends as a function of proton or neutron number. The calculated quadrupole moments and charge radii vary gradually with $Z$ and $N$, which would intuitively suggest strong inter-correlations.

The calculated CoD diagrams show patterns that are surprisingly localized as compared to the smooth trends of observables. These local variations of CoDs reflect the underlying deformed shell structure and changes of single-particle configurations due to crossings of s.p. levels, especially high-$N_{osc}$ intruder and oblate-driving extruder levels.

Our results suggest that the frequently made assumption of strong correlations between smoothly-varying observables, which must result in reduced statistical errors of their differences, cannot always be justified.